NUMERICAL SIMULATIONS ON INFLUENCES OF VARIATION OF SEA ICE THICKNESS AND EXTENT ON ATMOSPHERIC CIRCULATION*

WU Bingyi (武炳义), *HUANG Ronghui* (黄荣辉) and *GAO Dengyi* (高登义)

Institute of Atmospheric Physics, Chinese Academy of Sciences, Beijing 100029

Received January 4, 2002

ABSTRACT

By using a 2-layer AGCM designed by Institute of Atmospheric Physics, Chinese Academy of Sciences, this paper investigates influences of thickness and extent variations in Arctic sea ice on the atmosphere circulation, particularly on climate variations in East Asia. The simulation results have indicated that sea ice thickness variation in the Arctic exhibits significant influences on simulation results, particularly on East Asian monsoon. A nearly reasonable distribution of sea ice thickness in the model leads directly to stronger winter and summer monsoon over East Asia, and improves the model's simulation results for Siberia high and Icelandic low in winter. On the other hand, sea ice thickness variation can excite a teleconnection wave train across Asian Continent, and in low latitudes, the wave propagates from the western Pacific across the equator to the eastern Pacific. In addition, the variation of sea ice thickness also influences summer convective activities over the low latitudes including South China Sea and around the Philippines.

Effects of winter sea ice extents in the Barents Sea on atmospheric circulation in the following spring and summer are also significant. The simulation result shows that when winter sea ice extent in the target region is larger (smaller) than normal, (1) in the following spring (averaged from April to June), positive (negative) SLP anomalies occupy the northern central Pacific, which leads directly to weakened (deepened) Aleutian low, and further favors the light (heavy) sea ice condition in the Bering Sea; (2) in the following summer, thermal depression in Asian Continent is deepened (weakened), and the subtropical high in the northwestern Pacific shifts northward (southward) from its normal position and to be strengthened (weakened).

Key words: Arctic sea ice, thickness, East Asian monsoon, the Barents Sea, simulation

I. INTRODUCTION

Sea ice significantly influences variations of the atmospheric and oceanic circulation. As Ebert and Curry (1993) pointed out, variations of sea ice play a crucial role in climate via the following physical processes: (1) the formation of sea ice causes a much larger portion of the incoming solar energy to be reflected back to space. (2) the formation of sea ice reduces the transfer of sensible and latent heat between the ocean and atmosphere. (3) because of the latent heat associated with melting and freezing, sea ice acts as a thermal reservoir which delays the seasonal temperature cycle, and (4) the formation of sea ice

* This work was supported by the National Natural Science Foundation of China under Grant of No. 49905003.

alters the ocean salinity and hence the ocean density stratification by the expulsion of brine during freezing and by the large-scale transport of low-salinity ice.

Both thermodynamic and dynamic processes determine the extent and vertical thickness of sea ice. Actually, sea ice growth and heat transfer between the ocean and atmosphere are extremely influenced by sea ice thickness. In order to calculate the large-scale heat exchanges between the ocean and atmosphere, it should be known that distribution of sea ice thickness and relations between heat flux and thickness of sea ice. Thickness of sea ice also exhibits obviously interannual variations similar to its extent. for instance, McLaren et al. (1995) suggested that over a 34-year period (1958—1992), the mean thickness over the North Pole was 3.6 m but demonstrated a large interannual variability, ranging from 2.8 in 1986 to 4.4 m in 1970. At present, however, much fewer researches have focused on the distribution of sea ice thickness except for thickness simulations by using a sea ice model. Therefore, on this condition, it is the best way to investigate effects of variations of sea ice thickness on atmospheric circulation by using an AGCM.

Treatment of sea ice thickness in AGCM mainly includes the following aspects: (1) a uniform thickness, for example, it is 2 m for NCAR CCM1 and 3 m for OSU and IAP (Institute of Atmospheric Physics, Chinese Academy of Sciences) model. (2) sea ice thickness is specified to vary linearly from 1 m at the edge of sea ice to 5 m at the North Pole (Hansen et al. 1983). (3) the seasonal contour maps of sea ice thickness (Bourke and Garrett 1987) were digitized to the latitude-longitude grid of the GISS model, and interpolated to the individual months (Rind 1995), and (4) the AGCM contains thermodynamic and dynamic processes of sea ice (McFarlane et al. 1992; Starley and Pollard 1995), therefore, sea ice thickness is also a prediction variable.

From the analyses mentioned above, it is evident that treatment processes about sea ice thickness in AGCM become more and more complicated, but less attention is paid to effects of those treatment processes on atmospheric circulation. In the present study we mainly focus on the influence of an unevenly distribution of sea ice thickness on atmospheric circulation, particularly on East Asian monsoon.

The previous studies about influences of sea ice extents on atmosphere circulation mainly emphasized the simultaneous effects (Herman and Johnson 1978; Yang and Huang 1992; Yang et al. 1993; 1994). Authors do not give unnecessary details for the progresses. In this paper, we study the lag influences of winter sea ice extents in the Barents Sea on atmospheric circulation.

II. PHYSICAL PROCESSES ASSOCIATED WITH SEA ICE AND EXPERIMENT SCHEMES

The model employed in this work is a 2-layer AGCM and developed by IAP, Chinese Academy of Sciences. The horizontal resolution is $4°\times 5°$ in latitude and longitude. The upper and lower levels are approximately at 400 hPa and 800 hPa respectively. For the details of the model, readers can be referred to Zeng et al. (1989).

The physical processes associated with sea ice in IAP model mainly include two aspects: one is sea ice albedo; the other is the conduction heat flux related with sea ice thickness. In IAP model:

$$\alpha_s = \begin{cases} \alpha_{sb} + s^{\frac{1}{2}}(\alpha_{sc} - \alpha_{sb}), & s < s_c = 1\ \mathrm{g/cm^2} \\ \alpha_{sc}, & s > s_c \end{cases} \tag{1}$$

where s is snow mass. α_{sc} and α_{sb} are the surface albedo with and without snow cover respectively. here. $\alpha_{sb}=0.45$ for sea ice and $\alpha_{sc}=0.8$ for snow cover.

The ground temperature for non-water surface is determined by the surface heat balance:

$$\Gamma \frac{\partial T_g}{\partial t} = S_4 - R_4 - LE_s - H_s - Q_d, \tag{2}$$

where S_4 is the solar radiation absorbed by the surface. R_4 the net upward long-wave radiation flux at the surface. LE_s the surface latent heat flux. H_s the surface sensible heat flux. and Q_d is the conduction heat flux at an infinitesimal distance below the surface. In Eq. (2). we have

$$\Gamma = \left(\frac{2kc}{\Omega}\right)^{\frac{1}{2}}, \tag{3}$$

where k is the value of the thermal conductivity (5.4×10^{-3} cal $\mathrm{cm^{-1}\ s^{-1}\ K^{-1}}$ for sea ice). c the specific volumetric heat capacity (0.45 cal $\mathrm{cm^{-3}\ K^{-1}}$ for sea ice). and Ω the diurnal frequency (rotation rate). The conduction heat flux Q_d at depth d is equal to zero except for sea ice. for which it is defined as

$$Q_d = \frac{k_{ice}}{D}(T_g - T_d), \tag{4}$$

where D (prescribed as 3 m) is sea ice thickness and $T_d=271.5$ K the surface temperature below the ice. If the predicted T_g for land or sea ice exceeds the melting temperature T_{ice}, then T_g is set equal to T_{ice} and the ice is implicitly assumed to melt since there is no ice mass budget equation in the model.

1. *Experiment Scheme for Sea Ice Thickness*

First, integration is performed with an uniform sea ice thickness (3 m) for 12 years, and each variable averaged from the 8-th to the 12-th year for each month stands for the corresponding climatology. Then, we run IAP 2L-AGCM continuously for 8 years by using specified sea ice thickness for each month, i. e., sea ice thickness varies linearly from 0.2 m at the edge of sea ice to 3.5 m at the North Pole for each month (Fig. 1). Specified sea ice thickness in the model not only accords with the observational fact of 3.6 m at the North Pole, but also emphasizes the important role of the thin ice in heat transfer between the ocean and atmosphere, which as suggested by Aleksander (1984) that when sea ice thickness changes from 1 to 100 cm, heat flux variation is over 2 orders of magnitude.

2. *Experiment Schemes for Sea Ice Extent*

In the previous study, Wu (1997) also revealed the phenomenon that the lag effects of the previous winter sea ice extents in the Barents and Kara Seas on the subtropical high over the western Pacific during the following spring and summer. In this section, we utilize IAP 2L-AGCM to investigate the lag influences of winter sea ice extents in the Barents Sea on atmospheric circulation. Two experiments were designed with the sea ice

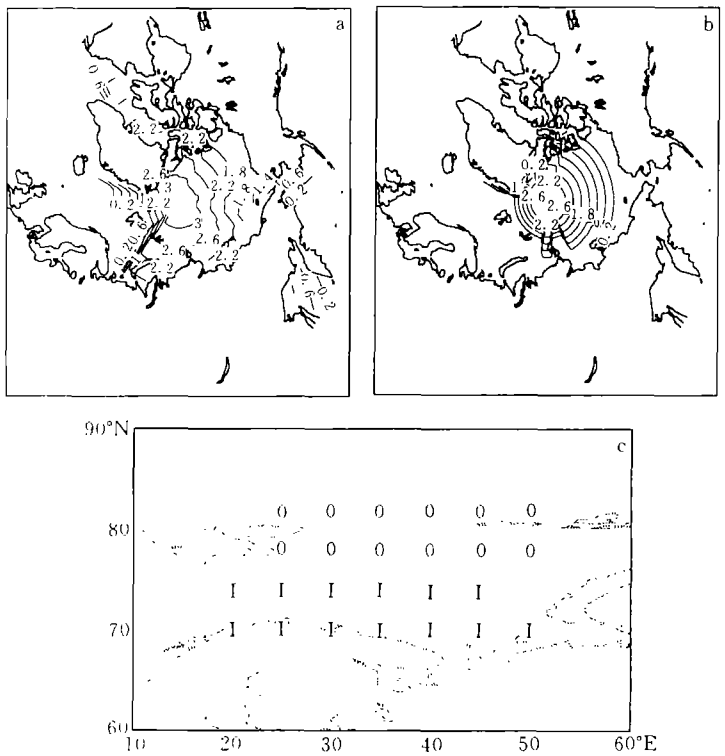

Fig. 1. The distribution of specified monthly mean sea ice thickness in (a) March and (b) September. Interval is 0.4 m. (c) The grid locations of specified winter (December, January and February) sea ice anomaly forcing, I: increased sea ice grids; 0: decreased sea ice grids.

extent anomalies in the region south of 82°N and 20°E to 60°E. Experiment 1 is for the heavy ice. Firstly, we run IAP model from January to November with the climatological sea ice extents, and then continuously run the model from December to February of the next year with increased sea ice extents (Fig. 1c) and from March to August of the next year with the climatological sea ice extents. Experiment 2 is for the light ice. The experiment is the same as in Experiment 1 except for decreased sea ice extents during December to February of the next year. Before performing the two experiments, we run the model from January to August of the next year in which integrating is going on without any change in physical conditions as a control experiment.

III. SIMULATION RESULTS

1. *Impacts of an Unevenly Distribution of Sea Ice Thickness on Atmospheric Circulation*

Figure 2a shows much of Asian Continent and the North Atlantic region, where sea level pressure (SLP) differences are positive, compared with the model's climatology, the simulations for winter Siberia high and Icelandic low are predominantly improved, winter Siberia high becomes stronger, and Icelandic low better approaches its climatology. Meanwhile, in the whole Arctic, northeastern Asia and much of Europe, SLP differences are negative. The distribution of SLP anomalies seems like EU teleconnection, this is an

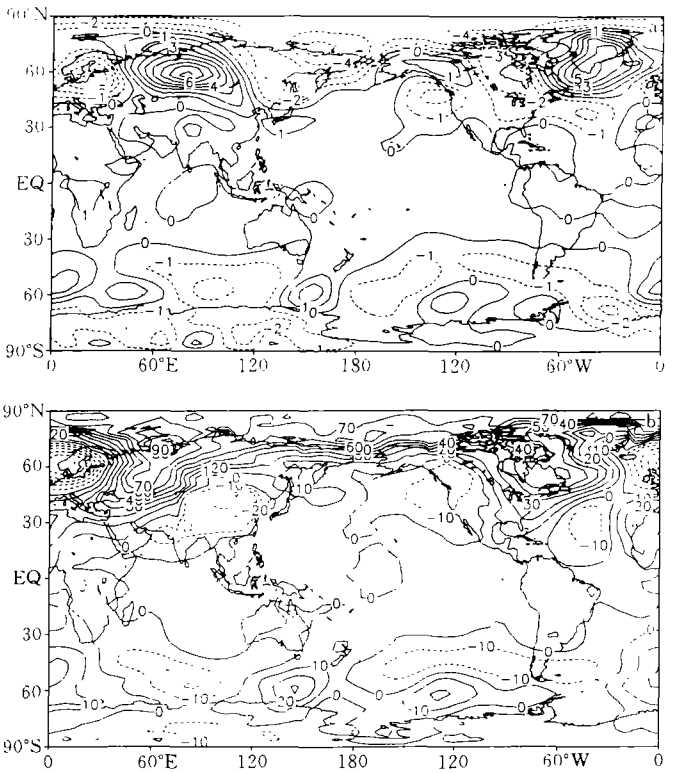

Fig. 2. The simulated winter (a) SLP (in hPa) and (b) 500 hPa height (in gpm) differences between the unevenly and the uniformly distribution of sea ice thickness simulation exepriment minus control experiment.

other feature to be noted. In fact, heat flux transfer from the ocean to atmosphere increases because the extent of thin ice is obviously lager than the previous. Therefore, SLP falls in a large part of Arctic, and accompanied SLP rises in some high-latitude regions. The largest height anomalies just centered at 60°E, northern 60°N with negative anomalies over East Asia cause a stronger meridional circulation, which is responsible for creating a stronger winter monsoon over East Asia (Fig. 2b). At 850 hPa wind fields, northerly anomalies prevail over East Asia, and extend southward to nearly 10°N, and convective activities around the southern Philippines tend to be stronger due to convergence in wind fields (Fig. 3).

In summer, thermal depression over Asian Continent is obviously deepened (Fig. 4a), particularly over the central China, and negative SLP anomalies extend to the northwestern Pacific, accompanying positive SLP anomalies over northern Pacific. Stronger blocking highs at 500 hPa emerge in the northern Okhotsk and Ural region, and meanwhile, the subtropical high over western Pacific tends to be also stronger and shifts northward (Fig. 4b). The phenomena appearing in both at SLP and 500 hPa imply that summer monsoon over East Asia tends to be strengthened.

In June, SLP anomalies (Fig. 5a) show that anomalies including the strengthened thermal depression over Asian Continent, negative SLP anomalies over the northwestern

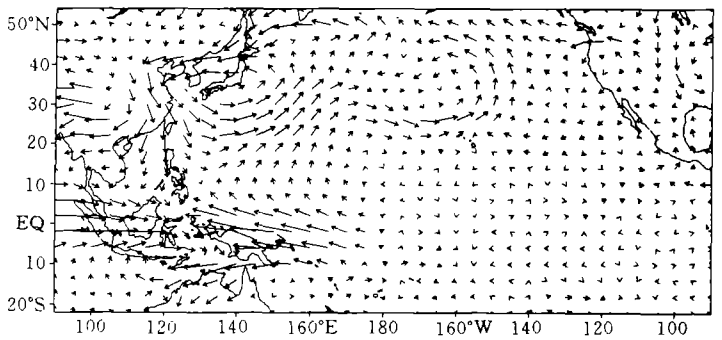

Fig. 3. Simulated winter wind anomalies at 850 hPa. Unit: m/s.

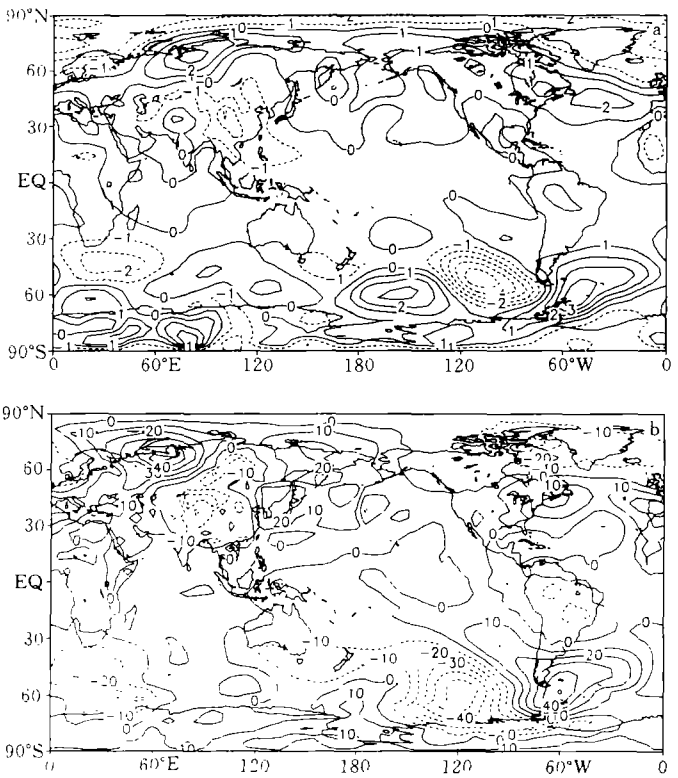

Fig. 4. As in Fig. 2, except for summer.

Pacific and positive SLP anomalies over the northern Pacific are directly favorable to a stronger summer monsoon over East Asia; another feature to be noted is that negative anomalies were separated from positive anomalies over the region between 20°S—20°N. The rainfall and diabatic heating would be increased corresponding to negative SLP anomalies. It can be seen (Fig. 5b) that the distribution of diabatic heating anomalies is very similar to that shown in Fig. 5a, and all the regions where SLP exhibits negative (positive) anomalies correspond to heating (cooling) in atmosphere. The largest diabatic

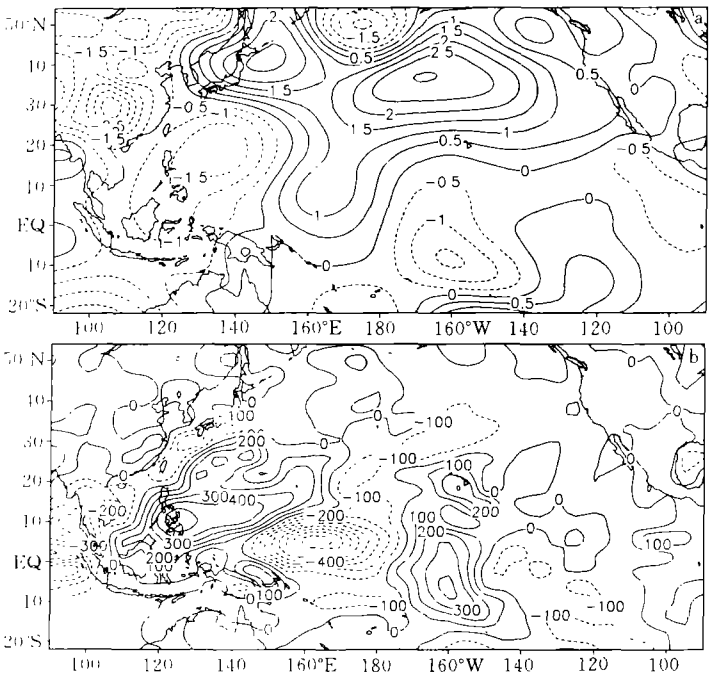

Fig. 5. The simulated June SLP differences (in hPa) (a) and diabatic heating anomalies (in 10^{-1} J/d) (b).

heating centered over the Philippines Sea implies convective activities to be more active. The distribution of velocity potential anomalies shown in Fig. 6, firstly, confirms that convergences in lower levels and divergences in upper levels well correspond to negative SLP anomalies; secondly, clearly exhibits wave-train structure extending from northern China to eastern Pacific, implying disturbances from the high-latitude propagate southeastward. In summer, the distribution of velocity potential anomalies (figure omitted) is similar to that shown in Fig. 6.

Figure 7 displays the latitude-time section of anomalous variables. It is clearly that SLP anomalies propagate from the high-latitude to the low latitude before June, and then positive anomalies move northward (Fig. 7a). The interesting phenomena are the propagation of positive and negative SLP anomalies with 30—60 day intervals. The time revolutions of height anomalies at 500 hPa (Fig. 7b) also exhibit similarities. Based on the above analyses, a more reasonable distribution of sea ice thickness in the model not only influences atmospheric circulation over the high-latitude and East Asia, but also affects convective activities over the low-latitude, and further changes the strength and location of the Walker circulation. Through the simulation experiment mentioned above, it indeed brings significant influences on the simulation results so as to change spatial distribution of sea ice thickness. Zhao (1992) summarized the results by using different AGCMs to simulate influences of the heavy ice-snow on climatic anomalies in the monsoon regions. Although the used AGCMs and anomalous experiments are different, the similar results indicate that the heavy ice-snow causes weaker thermal depression over Eurasian Continent in summer, and SLP is 10—25 hPa higher than normal, corresponding to weaker summer

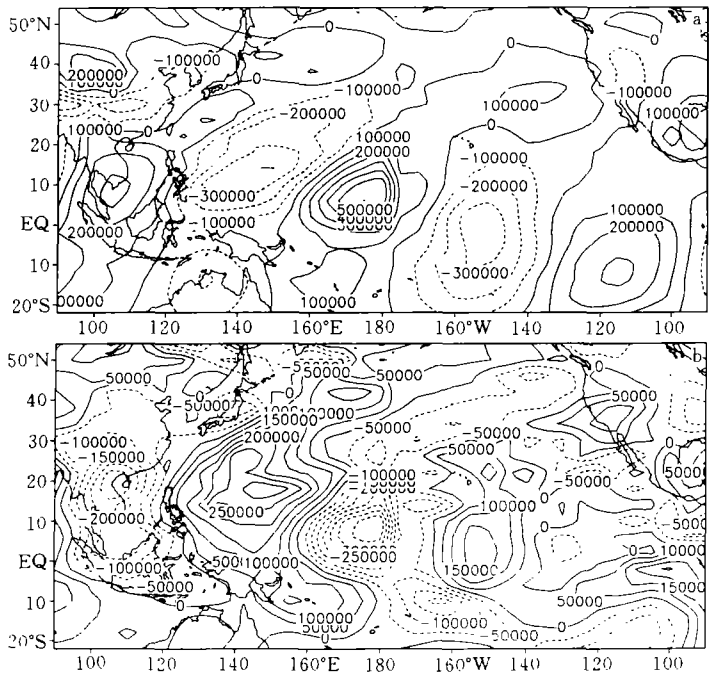

Fig. 6. The simulated distribution of June velocity potential anomalies (in $m^2 s^{-1}$) at (a) 850 hPa and (b) 400 hPa.

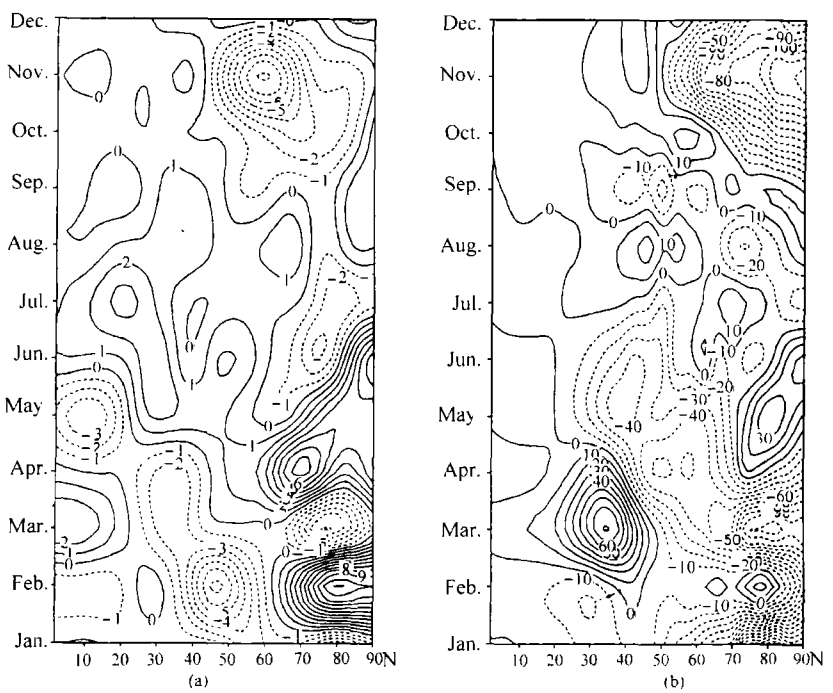

Fig. 7. The simulated latitude-time section of (a) SLP anomalies (in hPa) at 110°E, and (b) 500 hPa height anomalies (in gpm) at 125°E.

monsoon circulation. On the contrary, during the light ice-snow Asian summer monsoon circulation becomes stronger. Those are well coincident with our results.

2. *Lag Effects of Winter Sea Ice Extent in the Barents Sea on the Following Atmospheric Circulation*

Corresponding to the icy winter in the Barents Sea, in the following June, negative SLP anomalies cover much of Eurasian Continent with the largest negative anomalies near the Tibetan Plateau (Fig. 8a), while positive anomalies occur over northern Pacific. Therefore, summer monsoon would be stronger over East Asia. At 500 hPa (Fig. 8b), positive height anomalies occupy the northern Pacific and the south part of Asian Continent, and cause a strengthened subtropical high over the western Pacific. Height anomalies in the following summer also show the similar features (omitted). The phenomena indicate that the extent of subtropical high over western Pacific tends to be larger and shifts westward from its normal position corresponding to the previous icy winter in the Barents Sea.

In addition, Fig. 9a displays clearly that there are positive SLP anomalies over the region 30—60°N and 120—180°W with negative anomalies over much Asian Continent. At 500 hPa height fields (Fig. 9b), positive height anomalies cover the northeastern Pacific with large values exceeding 20 gpm, while weaker negative anomalies occur the south part of the Okhotsk Sea, those anomalies indicate that Aleutian low tends to be weaker than

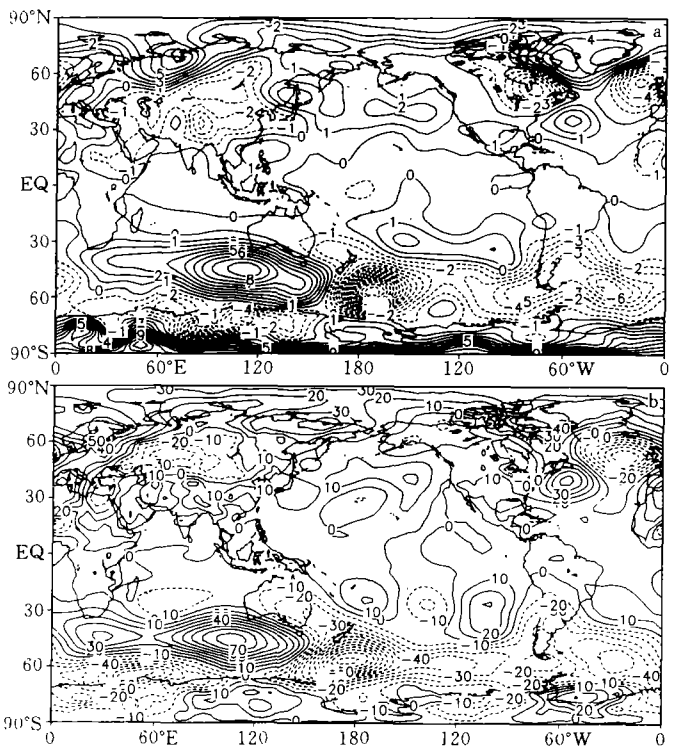

Fig. 8. The simulated (a) SLP anomalies, and (b) 500 hPa height anomalies in the following June for the heavy sea ice (Experiment 1 minus control run).

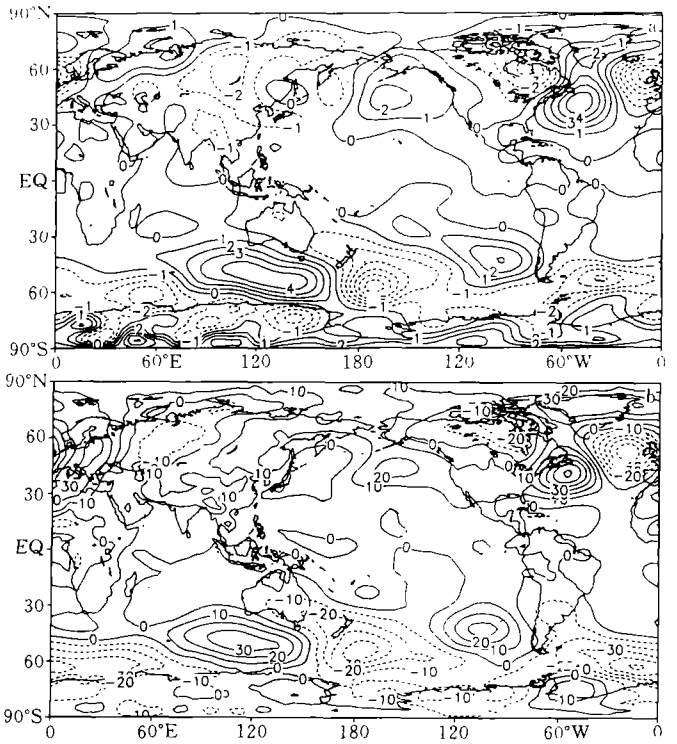

Fig. 9. As in Fig. 8, except for averaged from the following April to June.

normal and moves westward. In the previous study (Wu et al. 1999), we concluded the following results: winter sea ice extent in the Kara and the Barents Seas can affect SST in the northern Pacific in the following June, i. e., when the icy winter emerges in the sea regions, the weakened Aleutian low shifts westward from its normal position, and causes that cold air over the high-latitude frequently bursts out southward to influence SST in the central northern Pacific. Meanwhile, the study also revealed the inverse relation between winter sea ice extent in the Kara Sea, the Barents Sea and that in the Bering Sea in the following spring. The simulation results here demonstrate that the weakened Aleutian low and its moving westward completely result from the previous icy winter in the Barents Sea. At SLP fields, the southeast part of the Bering Sea has positive SLP anomalies and its west part is negative anomalies. Those anomalies lead to southerly anomalies over the region, and are favorable to the light sea ice. Nierauer (1980; 1988) analyzed interannual variations of sea ice in the Bering Sea, and suggested, that winter sea ice is mainly controlled by Aleutian low.

Since March the dominant feature is positive height anomalies covering much of the region 90—180°E except for May and June (Fig. 10a). In the middle latitudes (Fig. 10b), positive anomalies first emerge over 0—60°E in February, and then the anomalies slowly propagate in directions of the west and the east. The westward propagation of anomalies can reach 60°W in the following April, and the other continuously extends to east, and reaches near 170°E in the following August. Therefore, winter heavy ice in the Barents Sea not only influences the subtropical high over the northwestern Pacific, but also

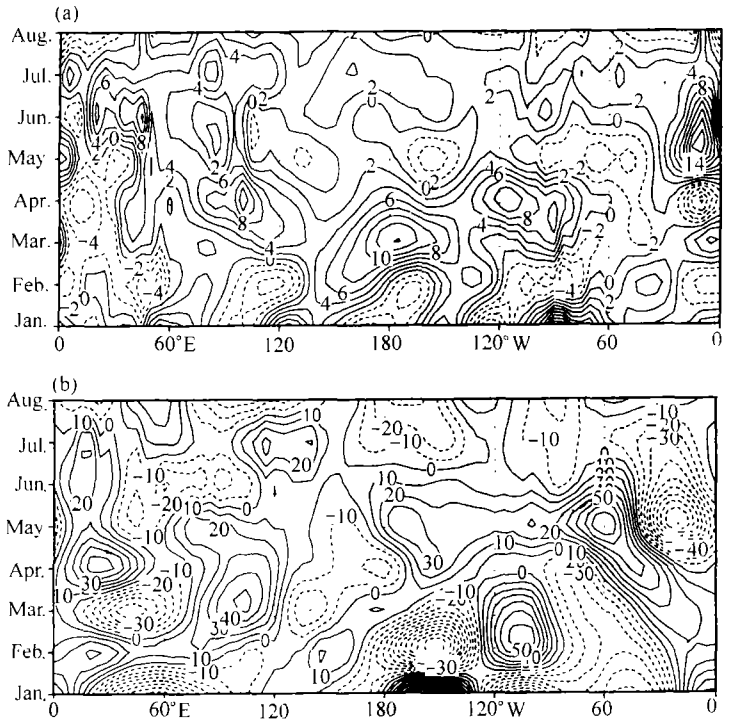

Fig. 10. The simulated longitude-time sections of height anomalies at 500 hPa for latitudes: (a) averaged from 6 to 22°N, (b) averaged from 46 to 50°N.

influences another one over the North Atlantic sector. In the previous study (Gao and Wu 1998), we revealed a close relation between winter sea ice extent in the Kara and the Barents Seas and the subtropical high in the following spring and summer over the North America and the North Atlantic sector. The simulation results here further confirm that the relation is true.

The general feature in height anomalies over the Northern Hemisphere is positive and negative anomalies propagating from high-latitudes to low-latitudes (Fig. 11a). After May, northward propagation from the low latitude becomes stronger. In the east of the data line, anomalies clearly exhibit northward propagation (Fig. 11b).

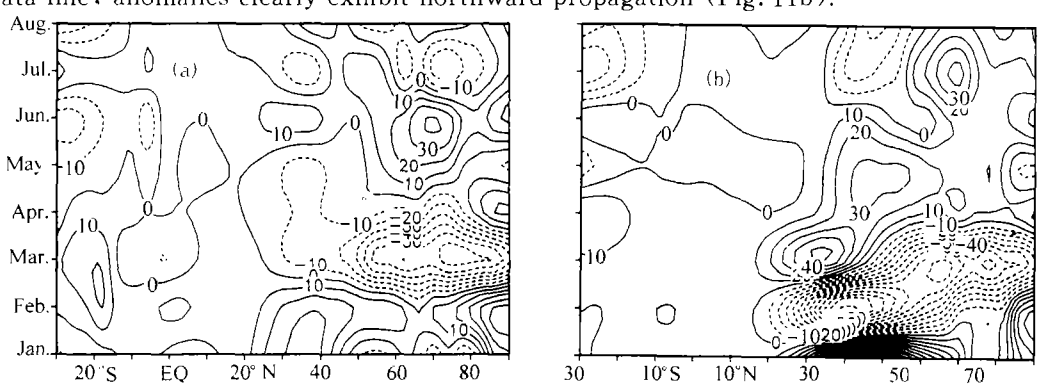

Fig. 11. The simulated latitude-time section of height anomalies at 500 hPa along (a) 145°E and (b) 160°W.

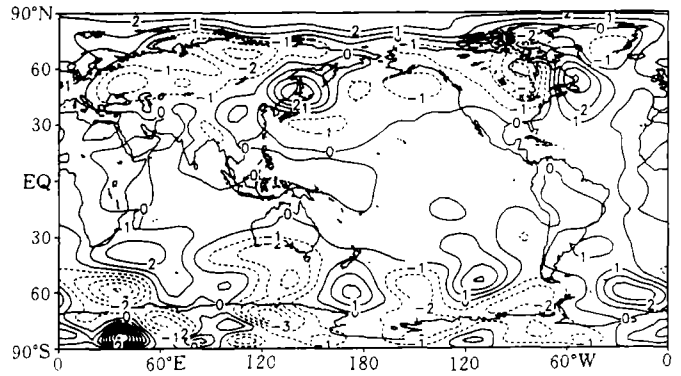

Fig. 12. As in Fig. 8a, except for averaged from the following April to June and light sea ice.

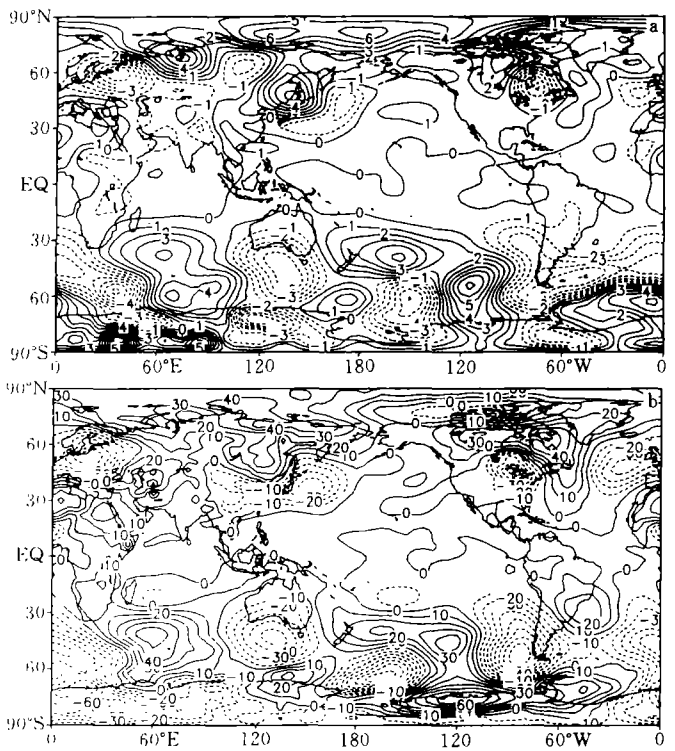

Fig. 13. As in Fig. 8, except for the light sea ice.

Through performing Experiment 2, we obtain effects of the light sea ice on the atmospheric circulation. In anomalous SLP fields averaged for the following period from April to June (Fig. 12), anomalies directly cause frequent cold air activities around the Aleutian region. Therefore, more than normal sea ice in the Bering Sea might be frozen. In the following June, positive anomalies occupy the South China Sea and around the marinetime (Fig. 13a), which means weaker convective activities over the region. At 500 hPa negative height anomalies cover East Asia and northwestern Pacific (Fig. 13b). The general features in the following summer also display similarities (figure omitted).

The revolutions of height anomalies at 500 hPa (Fig. 14) show westward propagation

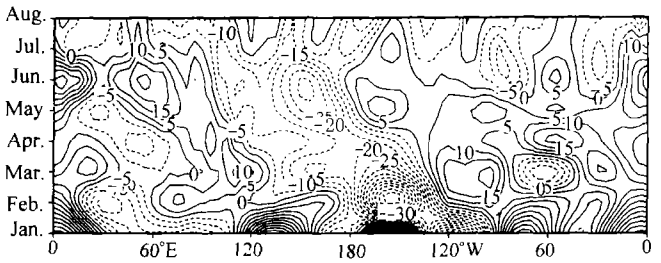

Fig. 14. The simulated longitude-time section of height anomalies at 500 hPa averaged from 26°N to 38°N for the previous light ice winter.

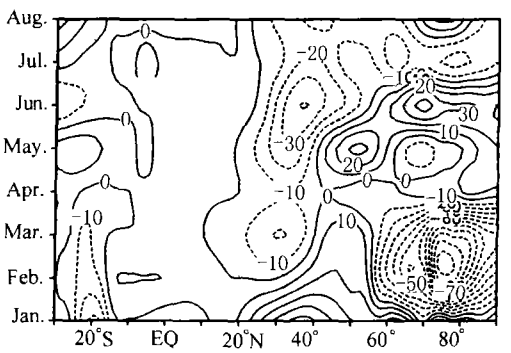

Fig. 15. As in Fig. 11a, except for the light sea ice.

over the northern Pacific and Asian Continent. The phenomenon obviously differs from that shown in Fig. 10a where positive anomalies propagate eastward over middle-latitudes. The other feature shown in Fig. 14 is negative anomalies over East Asia and the northern Pacific lasting from spring to summer, meaning that the subtropical high over the western Pacific is continuously weaker than normal. Figure 15 further confirms that this conclusion is true, i. e., negative anomalies are continuously maintained in middle latitudes.

IV. CONCLUSIONS AND DISCUSSION

The simulation results indicate that sea ice thickness variation in the Arctic exhibits significant influences on simulation results, particularly on East Asian monsoon. A nearly reasonable distribution of sea ice thickness in the model leads directly to stronger winter and summer monsoon over East Asia, and improves the model's simulation results for Siberia high and icelandic low in winter. On the other hand, sea ice thickness variation can excite a teleconnection wave train across Asian Continent, and in the low latitude, the wave propagates from the western Pacific across the equator to the eastern Pacific. In addition, the variation of sea ice thickness also influences summer convective activities over the low latitude including South China Sea and around the Philippines. In order to improve simulation results for East Asia monsoon, we should pay more attention to influences from sea ice thickness variations.

Effects of winter sea ice extents in the Barents Sea on atmospheric circulation in the following spring and summer are also significant. The simulation result shows that when winter sea ice extent in the target region is larger(smaller) than normal, two cases will

occur. (1)In the following spring(averaged from April to June), positive(negative)SLP anomalies occupy the northern central Pacific, which leads directly to weakened (deepened) Aleutian low, and further favors the light (heavy) sea ice condition in the Bering Sea; (2) in the following summer, thermal depression in Asian Continent is deepened (weakened), and the subtropical high in the northwestern Pacific shifts northward (southward) from its normal position and to be strengthened(weakened).

In addition, there is more winter sea ice in the Barents Sea, 500 hPa heights display positive anomalies over the low latitude in the western Pacific during the following spring to summer. In the middle latitude, positive height anomalies over the North Atlantic sector and Eurasian Continent show propagation feature in directions of the west and the east, and further influence the subtropical high over the North Atlantic sector during the following spring to summer.

Analyses mentioned above indicate that Arctic sea ice variations (extents and thickness) exhibit close association with climate variations in the northwestern Pacific and the North Atlantic sector. These associations are true because the simulation results here are well coincident with that from data analyses. The inherent problem in this approach is that a non-interactive ice-atmosphere system is assumed, i. e., the atmosphere is not allowed to change sea ice. In addition, the present study emphasizes the importance of sea ice variations in the Barents Sea. A natural question is what process determines sea ice variations in the target region? Wu et al. (2001) suggested that winter sea ice variations in the Kara and the Barents Seas are mainly influenced by the North Atlantic Warm Current. It should be pointed out that this paper used a 2-layer AGCM, and both of the vertical and the horizontal resolutions in the model are rough for investigating some deeply physical processes of sea ice feedback to atmosphere.

REFERENCES

Aleksandr, P. M. (1984), The heat budget of Arctic ice in the winter, Arctic and Antarctic Research Institute, 46—62.

Bourke, R. H. and Garrett, R. P. (1987), Sea ice thickness distribution in the Arctic Ocean, *Cold Reg. Sci. Technol.*, **13**: 259—280.

Ebert, E. E. and Curry, J. A. (1993), An intermediate one-dimensional thermodynamic sea ice model for investigating ice-atmosphere interactions, *J. Geophys. Res.* **98**(C6): 10085—10109.

Gao Dengyi and Wu Bingyi (1998), A preliminary study on decadal oscillation and its oscillation source of sea-ice-air system in the Northern Hemisphere, *Polar Meteorology and Glaciology*, **12**: 68—78 (in Chinese).

Hansen, J. E. et al. (1983), Efficient three-dimension global models for climate studies: Models I and II, *Mon. Wea. Rev.*, **111**: 609—662.

Herman, G. F. and Johnson, W. T. (1978), The sensitivity of the general circulation to Arctic sea ice boundaries: A numerical experiment, *Mon. Wea. Rev.*, **106**: 1649—1664.

McFarlane, N. A. et al. (1992), The Canada climate center second generation general circulation model and its equilibrium climate, *J. Climate*, **15**: 1013—1045.

McLaren, A. S. et al. (1995), Variability in sea ice thickness over the North Pole from 1958 to 1992, *The Polar Oceans and Their Role in Shaping the Global Environment*, 363—371.

Niebouer, H. J. (1980), Sea ice and temperature variability in the Eastern Bering Sea and the relation to

atmospheric fluctuation, *J. Geophys. Res.*, **85**: 7507—7515.

Niebouer, H. J. (1988), Effects of El Nino-Southern Oscillation and North Pacific weather pattern on interannual variability in the subarctic Bering Sea, *J. Geophys. Res.*, **93**: 5051—5068.

Rind, D. (1995), The role of sea ice in $2\times CO_2$ climate model sensitivity, Part I : The total influence of sea ice thickness and extent, *J. Climate*, **8**: 449—463.

Starley, L. T. and Pollard, D. (1995), A global climate model (GENESIS) with a land-surface transfer scheme (LSX), Part I: Present climate simulation, *J. Climate*, **8**: 732—761.

Wu Bingyi (1997), Study on Arctic sea ice variations and its influences on climate variations over the East Asia and the Northern Hemisphere, Thesis, Institute of Atmospheric Physics, Chinese Academy of Sciences (in Chinese).

Wu Bingyi, Huang Ronghui and Gao Dengyi (1999), The effects of winter sea-ice variation in the Kara/Barents Seas on the SST in the Northern Pacific in following spring, *Climatic and Environmental Research*, **4**: 165—175 (in Chinese).

Wu Bingyi, Huang Ronghui and Gao Dengyi (2001), Arctic sea ice bordering on the North Atlantic and interannual climate variations, *Chinese Science Bulletin*, **46**: 162—165.

Yang Xiuqun and Huang Shisong (1992), Numerical experiment of climatic effect of Antarctic sea ice during the Northern Hemisphere summer, *Chinese J. Atmos. Sci.*, **16**: 80—89.

Yang Xiuqun, Xie Qian and Huang Shisong (1993), Numerical experiment of influences of ice and snow disappearance in the Antarctic on atmosphere circulation and climate, *Acta Geographica Sinica*, **48**: 394—401 (in Chinese).

Yang Xiuqun, Xie Qian and Huang Shisong (1994), Numerical experiment of influences of Arctic sea ice anomaly on Asia summer monsoon, *Acta Oceanologica Sinica*, **16**: 34—40 (in Chinese).

Zeng Qincun et al. (1989), Documentation of IAP two-level AGCM, TR004, DOE/ER/60314—H1, U.S. DOE., 383pp.

Zhao Zongci (1992), Numerical simulations on roles of the ocean in climate variation, *Proceedings of the Regulation and Control Roles From the Ocean on Climate Variations*, Edited by National Oceanological Bureau, Beijing, China Oceanological Press, 206pp. (in Chinese).